

<Cover page>

Comparative analysis for tumorigenesis  
of human papillomavirus according to  
anatomic sites in squamous cell  
carcinoma of the head and neck

Sei Young Lee

Department of Medicine

The Graduate School, Yonsei University

<Title page>

Comparative analysis for tumorigenesis  
of human papillomavirus according to  
anatomic sites in squamous cell  
carcinoma of the head and neck

Directed by Professor Eun Chang Choi

The Doctoral Dissertation  
submitted to the Department of Medicine,  
the Graduate School of Yonsei University  
in partial fulfillment of the requirements for the degree  
of Doctor of Philosophy

Sei Young Lee

June 2007

<Signature page>

This certifies that the Doctoral  
Dissertation of Sei Young Lee is  
approved.

-----  
-----  
-----  
-----  
-----

The Graduate School  
Yonsei University

June 2007

## ACKNOWLEDGEMENTS

I owe an enormous depth of gratitude to Prof. Eun Chang Choi who has guided me through this thesis with invaluable advice and delicate attention. I also extend thanks to Prof. Won Young Lee, Prof. Nam Hoon Cho, Prof. Se Heon Kim and Prof. Jae Ho Cho, who have not spared any professional suggestion for improvement. My heartfelt thanks go to researchers in the pathology lab. They have participated in my experiments like their own and always made themselves available to answer my numerous questions.

Finally, I dedicate this thesis to my parents whose support and sacrifice have led my life to this date and my wife, You-Ree and daughters for their infinite love and encouragement.

## <TABLE OF CONTENTS>

ABSTRACT .....	1
I. INTRODUCTION.....	3
II. MATERIALS AND METHODS .....	5
1. Selection of tissue samples and DNA extraction .....	5
2. HPV genotyping .....	5
3. Real-time PCR .....	6
4. Tissue microarray .....	7
5. Immunohistochemistry .....	8
6. Fluorescent in situ hybridization .....	8
7. Statistical analysis .....	9
III. RESULTS .....	11
1. HPV prevalence in head and neck cancers .....	11
2. Investigation of viral physical status in head and neck cancers .....	11
3. Molecular comparison according to HPV infection in palatine tonsillar cancer .....	15
4. Pathologic correlation according to HPV infection in head and neck cancers .....	19
5. Clinical correlation according to HPV infection in head and neck cancers .....	27
IV. DISCUSSION .....	28
V. CONCLUSION .....	32
REFERENCES .....	34
ABSTRACT(IN KOREAN) .....	38

## LIST OF FIGURES

Figure 1. Comparison of PCR amplification efficiencies for HPV-16 E2 and E6 .....	13
Figure 2. Immunohistochemical results from tissue microarray .....	18
Figure 3. Fluorescent in situ hybridization (FISH) .....	19
Figure 4. Microscopic differences between tonsillar cancer of surface origin and crypt origin.....	20
Figure 5. Microscopic findings to suggest a cryptal origin for tonsillar cancer .....	21
Figure 6. Histopathologic findings associated with vocal cord motility or fixation .....	22
Figure 7. Invasive depth of glottic carcinoma .....	23
Figure 8. Invasive pattern in the thyroid cartilage with glottic cancer .....	24
Figure 9. Invasive pattern in the stroma with tongue cancer .....	25
Figure 10. Lymphovascular and perineural invasion in early-onset tongue cancer .....	26
Figure 11. Comparison of invasion characteristics according to	

HPV infection in the early stage of tongue cancer .....	26
Figure 12. Comparison of tumor-specific survival according to HPV infection .....	27

## LIST OF TABLES

Table 1. Comparative prevalence of HPV in head and neck cancer .....	11
Table 2. Physical status of HPV-16 infection in palatine tonsillar cancer and tonsillitis patients .....	13
Table 3. Physical status of HPV-16 infection in glottic cancer and tongue .....	15
Table 4. Association of p16 and c-myc with clinicopathological parameters .....	17

<ABSTRACT>

Comparative analysis for tumorigenesis of human papillomavirus according to anatomic sites in squamous cell carcinoma of the head and neck

Sei Young Lee

*Department of Medicine*  
*The Graduate School, Yonsei University*

(Directed by Professor Eun Chang Choi)

The human papillomavirus (HPV) infection has caused controversy as a causative factor for head and neck cancers, despite the relatively high frequency of HPV infection in extragenital organ cancers. HPV infection of oropharyngeal mucosal regions most commonly affects the tonsil. We aimed to examine the association of HPV with palatine tonsillar cancers (PTC), glottic cancers (GC), and tongue cancers (TC) in order to clarify whether HPV directly affects the oncogenesis and biologic behavior of head and neck cancers. Furthermore, we attempted to correlate HPV infection with pathologic differences and clinical implications. We observed a significant difference in HPV prevalence among the cancers examined; HPV was detected in 73.1% (38/52), 7.4% (7/95), and 36.1% (13/36) of PTC, GC, and TC patients, respectively. Of the HPV-positive tumors in head and neck cancer, HPV-16 is the single most common type. The remaining tumors were infected by non-16 high-risk types, such as HPV-18, 33, 35, and 58. GC and TC were occasionally associated with low risk types, 6 or 11, but none of the PTC patients were infected with a low-risk HPV type. HPV-16 was most consistently integrated in PTC samples, whereas it was



mostly episomal in GC. TC with HPV infection resulted in less stromal invasion and a favorable outcome. HPV-16 integration may be directly related to PTC carcinogenesis, which initiates in the tonsillar crypts, and to early-onset TC, whereas HPV appears to be coincidentally associated with GC.

---

Key words : human papillomavirus, squamous cell carcinoma, tonsil, tongue, glottis

Comparative analysis for tumorigenesis of human papillomavirus  
according to anatomic sites in squamous cell carcinoma of the head and  
neck

Sei Young Lee

*Department of Medicine*  
*The Graduate School, Yonsei University*

(Directed by Professor Eun Chang Choi)

## **I. INTRODUCTION**

Human papilloma virus (HPV) may play a role in the pathogenesis of head and neck cancers, including palatine tonsillar cancer (PTC), glottic cancer (GC), and tongue cancer (TC), given the similarities in morphology and in susceptibility to HPV exposure between the tissues involved in head and neck cancers and cervical cancer. HPV infection is prevalent in the oropharyngeal mucosal regions, and the tonsil is the most commonly affected anatomical region in the oropharynx.<sup>1-3</sup> Furthermore, cancers involving those sites frequently have a verrucous or papillomatous appearance with tumor cells occasionally showing features of HPV infection, namely koilocytotic atypia. Furthermore, the glottis has a transition zone similar to that in the uterine cervix and the oral tongue may be the first site to exposure to virus in aerodigestive tract. However, it still remains uncertain whether HPV is directly associated with the malignant transformation of oral, oropharyngeal or laryngeal tumors.

The molecular biology of viral oncogenesis is well established. The viral protein E6 promotes the degradation of p53 and E7 inactivates pRb, usually followed by viral integration into the host genome.<sup>4,5</sup> For viral integration, disruption occurs most frequently in the E2 open reading frame (ORF), with the E1 ORF being disrupted in only a minor proportion of patients. Both ORFs are important in viral replication and transcription. More specifically, the breakage of E2 allows for the misregulation of the E6/E7 oncoprotein, which eventually leads to a malignant transformation.<sup>6</sup> In the non-integrated episomal state, the transcriptional level of E6/E7 is regulated by a promoter in the long control region in high-risk HPV-infected cells. Transcription of E6/E7 is also influenced by viral and cellular transcription factors, including the binding sites for the transcription factor Yin Yang 1 (YY1).<sup>7</sup> An investigation of the physical status of HPV would be helpful in finding a link between the virus and carcinogenesis of head and neck cancers. Squamous cell carcinoma (SCC) of the glottis represents one of the most common locations of all laryngeal SCC.<sup>2</sup> The most frequently reported risk factors for larynx cancer are smoking and alcohol, and genetic susceptibility is associated with polymorphisms in enzymes implicated in the detoxification of alcohol and tobacco.<sup>1,8-9</sup> In a recent overview of HPV and laryngeal cancer, there were conflicting reports of HPV prevalence ranging from 3 to 85%, with HPV-16 being the most frequently isolated type. While not specifically evaluated in laryngeal cancer, it has been demonstrated that patients with HPV-positive head and neck cancer demonstrate better survival rates than those with HPV-negative cancers.<sup>10</sup>

We aimed to clarify whether HPV directly affects the oncogenesis and biologic behavior of head and neck cancers by analyzing the HPV prevalence, physical state of the virus, and clinicopathologic prognostic factors in oral, oropharyngeal and laryngeal squamous cell carcinomas.

## **II. MATERIALS AND METHODS**

### **1. Selection of tissue samples and DNA extraction**

Samples from 52 patients were collected from the archived, paraffin-embedded tonsillar squamous cell carcinoma registry of Yonsei University Medical College Department of Pathology and Head and Neck Oncology Division of Otorhinolaryngology, from the period between 1995 and 2005. A total of 61 patients who underwent tonsillectomy for CFT were also selected as the control group.

Ten-micrometer sections were cut from paraffin blocks and collected in 1.5-ml Eppendorf tubes for DNA extraction. To prevent cross-contamination, each block was cut after a thorough cleaning of the microtome blade. Paraffin-embedded samples were placed in xylene for 5 min and centrifuged at 14,000 rpm. DNA extraction was carried out using the QiaAmp DNA minikit (Qiagen, USA, CA). The quality (ratio of 260/280 nm) and quantity (absorbance at 260 nm) of the isolated DNA were determined by optical density measurement. CasKi and SiHa cells were grown for approximately five days in the appropriate medium (CasKi cells and SiHa cells, RPMI 1600 [Gibco-BRL, Grand Island, N.Y.]). DNA isolation was performed with the QiaAmp DNA minikit according to the protocol for cultured cells grown in a monolayer.

### **2. HPV genotyping**

We used an HPV genotyping DNA chip (Biocore, Korea, Seoul) arrayed with multiple oligonucleotide probes of L1 sequences from 26 types of HPV, according to the manufacturer's protocol.<sup>11</sup> Consensus PCR products for L1 were hybridized to the arrayed probes on the HPV chip, and HPV genotypes were identified using a fluorescence scanner (GenPix 4000B, Axon Instruments Inc, USA, CA) with a 532-nm laser for excitation of Cy3. The fluorescence intensity data of the specific probes were then printed out as an Excel

spreadsheet.

### **3. Real-time PCR**

The copy numbers of the HPV E2 and E6 ORFs were assessed using a TaqMan-based 5'-exonuclease quantitative real-time PCR assay based on the DNA amplification of a 76-bp sequence of the E2 ORF and an 81-bp sequence of the E6 ORF in the presence of HPV-16 E2- and E6-specific hybridization probes, respectively.<sup>12</sup> The primers and probe for the E2 assay were designed to recognize the E2 hinge region of the E2 ORF, which is most often deleted upon HPV-16 integration in cervical carcinomas.<sup>13-14</sup> For each specimen, identical amounts of DNA were quantified for the E6 and E2 sequence of HPV-16. Each specimen was assayed three times. The PCR amplification was performed in a 25- $\mu$ l volume containing 1  $\times$  iQ SuperMix (BioRad, Hercules, CA), 200 nM E2 and E6 specific primers (Table 1), 100 nM dual-labeled (5'Hex and 3'BHQ2) E2 and (5'FAM and 3'BHQ1) E6 fluorogenic hybridization probe, and 200 ng of the genomic DNA template. All experiments were performed using the real-time iCycler™ PCR platform (BioRad, Hercules, CA). In each experiment, we included two standard curves obtained by amplification of a dilution series of the HPV viral copy number using CaSki (American Type Culture Collection, Manassas, VA) cell line genomic DNA, which is known to have 600 copies/genome equivalents (6.6 pg of DNA/genome).<sup>15-16</sup> There was a linear relationship between the threshold cycle values plotted against the log of the copy number over the entire range of dilutions. The amplification ramp included two hold programs of 2 min at 50°C and 10 min at 95°C, followed by a two-step PCR cycle with a melting step for 15 s at 95°C and an annealing step for 1 min at 60°C, for a total of 45 cycles. The ratio of E2 to E6 copy numbers was calculated to determine the physical status of the HPV-16 viral gene. HPV-16 in the pure episomal form is expected to have equivalent copy numbers to those of the E2 and E6 genes (i.e. E2/E6 ratio = 1), whereas preferential

disruption of E2 upon viral integration should result in fewer E2 gene copies than E6 genes. This means that an E2/E6 ratio of less than 1 would indicate the presence of both the integrated and episomal forms, while a ratio of 0 would indicate the presence of only an integrated form. The copy number of the integrated E6 gene was calculated by subtracting the copy number of E2 (episomal) from the total copy number of E6 (episomal and integrated). The ratio of E2 to integrated E6 genes represents the amount of the episomal form in relation to the integrated form. Values less than 1 indicate the predominance of the integrated form. DNA extracted from the cervical carcinoma cell line SiHa, known to harbor a pure, integrated form of the HPV-16 gene in which the E2 and E4 ORFs are disrupted, was used as the control for E2 (negative) and E6 (positive) amplification.<sup>17-18</sup> The relative viral load can be estimated by calculating the ratio of copies of E6 in the sample and in SiHa cells.

#### **4. Tissue microarray**

Recipient blocks were made from purified agar in 3.8 x 2.2 x 0.5-cm frames. Holes of 2 mm were made in the recipient blocks using a core needle, and the agar cores were discarded. The paraffin donor blocks were prepared after a thorough evaluation of the hematoxylin-eosin-stained slides. Every two adjacent areas of invasive carcinoma from the matching donor blocks were transplanted into the recipient blocks using a 2-mm core needle. The array for the cohort of patients with adjacent normal areas was constructed from paraffin-embedded, formalin-fixed tissue blocks. The recipient blocks were also framed in the mold that was used for the conventional paraffin block. Paraffin was then added to the frame. Consecutive 4- $\mu$ m-thick sections were cut from the recipient blocks using an adhesive-coated slide system (Instrumedics, Inc., New Jersey, USA).

## **5. Immunohistochemistry**

Four-micron sections were placed on silane-coated slides, deparaffinized, immersed in phosphate-buffered saline (PBS) containing 0.3% (v/v) hydrogen peroxide, and then processed in a microwave oven (10 mmol/L sodium citrate buffer, pH 6.5, for 15 minutes at 700W). After blocking with 1% (w/v) bovine serum albumin in PBS containing 0.05% (v/v) Tween-20 for 30 minutes, the slides were incubated overnight at 4°C with p16, survivin, HIF-1, skp-1, cyclin A, and cyclin B1. Immunoperoxidase staining was performed using the streptavidin-biotin peroxidase complex method (LSAB universal kit, DAKO, Carpinteria, CA). For negative controls, the antibodies were replaced with equivalent amounts of the subtype-matched normal mouse IgG. The final reaction product was visualized by the addition of 0.03% (w/v) of 3,3'-diaminobenzidine tetrachloride for 5-20 minutes. Strong nuclear staining, except in the cases of p16 and survivin with cytoplasmic diffusion, was considered positive. Immunostaining was graded and scored as follows: 0 (no staining), 1+ (weak and diffuse or strong and focal staining), 2+ (strong and diffuse staining). In addition, a three-tiered grading system was used for p16 which included 1+ (weak focal staining), 2+ (weak and diffuse or strong and focal staining), and 3+ (strong and diffuse staining).

## **6. Fluorescent in situ hybridization**

Two-color FISH was done on 3.5-micron consecutive sections from the same TMA paraffin blocks. Before hybridization, the sections were deparaffinized, air-dried and dehydrated in 100% ethanol after incubation at 56 °C for 24 h. TMA slides were treated in a wash buffer (Vysis Inc, Downers Grove, IL) for 3 min after treatment with 0.2N HCl for 20 min. The pretreatment solution (Vysis) at 80°C was applied for 30 min, and the slides were then washed with

purified water. Slides were treated with wash buffer twice for 5 min each. Protease solution (Vysis) was applied to the immersed slides at 37 °C for 10 min, and the slides were washed with a wash buffer and air-dried. Slides were fixed in 10% buffered formalin for 10 min and were washed with a wash buffer. Slides were immersed in denaturation solution (Vysis) for 5 min at 72 °C, followed by serial dehydration with 70%, 85%, and 100% ethanol. For c-myc hybridization, 20 1 mixed LSI c-myc and CEP8 probes (Vysis) were applied, and a coverslip was placed. After overnight hybridization at 37 °C in a humidified chamber, the slides were washed with a posthybridization wash buffer (Vysis) at 42 °C for 2 min. Nuclei were counterstained with 20 1 4, 6-diamino-2-phenylindole (Vysis). For HER2 hybridization, 20 1 LSI HER2/CEP17 probes (Vysis) were applied, and a coverslip was placed. After overnight hybridization at 37 °C in a humidified chamber, the slides were washed with a 72°C posthybridization wash buffer for 2 min. Nuclei were counterstained with 20 1 4, 6-diamino-2-phenylindole.

The c-myc and HER2 gene copy numbers in the tumor cells were estimated in approximately 200 nuclei in relation with centromere (CEP) 8 and CEP17. Hybridization signals were enumerated as the ratio of orange signals(c-myc and HER2) to green signals (CEP8 and CEP17) in morphologically intact and non-overlapping nuclei. At least a 3-fold increase of the c-myc signals over the CEP8 signals in the tumor cells was considered the criterion for gene amplification. The same criterion was applied to the HER2 amplification analysis using the LSI HER2 probe together with the CEP17 probe.

## **7. Statistical analysis**

The relationship between HPV status and clinicopathological parameters (TNM stage, recurrence, survival, origin of cancer, depth of invasion) or molecular factors (p16, cyclin A, cyclin B1, skp-1) were analyzed using



cross-tabulations and Fisher's exact test with SAS software, version 9.1 (SAS Institute Inc., Cary, NC, USA). Survivals of patients were calculated using the Kaplan-Meier method and curves were compared using the log-rank test. A p-value less than 0.05 was considered statistically significant.

### III. RESULTS

#### 1. HPV prevalence in head and neck cancers

In the present study, HPV was detected in 73.1% (38/52), 7.4% (7/95), and 36.1% (13/36) of the PTC, GC, TC patients, respectively (Table 1). Of the HPV-positive tumors in head and neck cancer, HPV-16 is the single most common type. The remaining tumors were infected by non-16 high-risk types, such as HPV-18, 33, 35, and 58. GC and tongue cancer were occasionally associated with the low risk types, 6 or 11, whereas none of the PTC patients were infected with low-risk type HPV. Among the 69 CFT specimens, HPV was detected in 8 samples (11.6%), of which 3 were found to have HPV-16 and the remaining 5 were infected by HPV-58 or low-risk types (HPV-6, 11 or 84). PTCs were found to be significantly associated with HPV infection ( $p < 0.0001$  by chi-squared)

**Table 1. Comparative prevalence of HPV in head and neck cancer**

	Tonsil cancer	Glottic Cancer	Tongue cancer	Total
Sample Number	52	95	36	183
HPV prevalence	73.1%	7.4%	36.1%	31.7%(58/183)
HPV-16	87.2%	60%	84.6%	83.6%(51/61)
Association with HPV infection	$P < 0.0001$	$P > 0.05$	$P > 0.05$	

#### 2. Investigation of viral physical status in head and neck cancers

Both validated assays of the real-time amplification systems for E2 and E6 ORFs using serially-diluted HPV-16 plasmid DNA showed similar amplification efficiencies, as reflected by the almost identical slopes of the

amplification curves (**Fig 1**). The results for the physical states and the copy numbers of HPV-16 E2 and E6 are summarized in **Table 2, 3**. Integrated E6 was calculated by subtracting the numbers of E2 from numbers of E6. The ratio of E2 to integrated E6 represents the amount of the episomal form relative to the integrated form. A value of less than 1.0 indicates a predominance of the integrated form.

When only the episomal form is present, equivalent copy numbers of E2 and E6 should be detected. This was found in two samples (5.9%) of 34 HPV-16-positive PTCs. Our data showed HPV-16 integration occurred in 94.1% of 34 HPV-16-positive PTCs. These included 14 specimens (41.2%) without detectable E2 sequences, which indicates the complete integration of viral genes into the host genome. There were also 18 specimens (52.9%) with an E2/E6 ratio between 0 and 1, which indicates the presence of a mixture of integrated and episomal forms. Among the 32 HPV-16 non-episomal status samples, 30 cases showed a predominance of the viral integrated form, with a ratio of E2 to integrated E6 of less than 1. Three samples of HPV-16-positive CFT patients showed purely episomal forms.

Of 11 TC samples with HPV-16 infection, 6 cases were integrated (54.5%), whereas HPV infection was present in only a minor proportion of glottic cancer, with integration in one case of 3 GC samples with HPV-16 infection(33.3%).

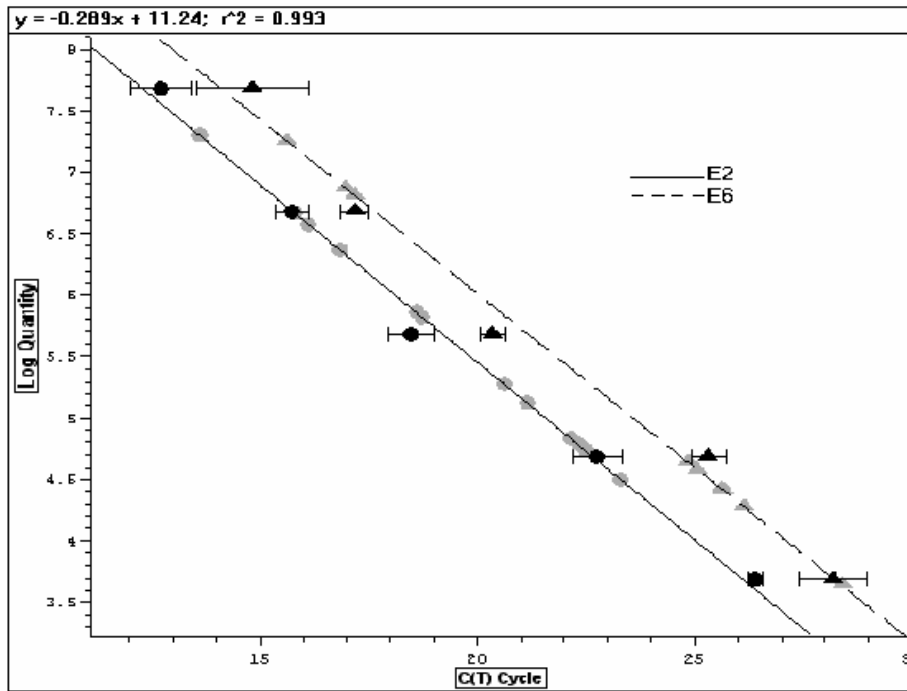


**Fig. 1. Comparison of PCR amplification efficiencies for HPV-16 E2 and E6.**  
 A 5-point 10-fold series of Caski cell line genomic DNA ( $2 \times 10^{-2}$  to  $2 \times 10^2$  ng) with amplification efficiencies was found to be very similar for the two reactions.

**Table 2. Physical status of HPV-16 infection in palatine tonsillar cancer and tonsillitis patients**

Dx / Origin	HPV-16 E6 copies	HPV-16 copies/cell	E2/E6 ratio	E2/integrated E6	Physical status
PTC-1/C	47610	0.29	0.03	0.03	Mixed (>Integrated)
PTC-2/M	39170	0.24	0.33	0.50	Mixed (>Integrated)
PTC-3/C	2495	0.01	0	0	Integrated
PTC-4/C	8749	0.05	0	0	Integrated
PTC-5/C	420000	2.58	0.05	0.06	Mixed (>Integrated)
PTC-6/C	34750	0.21	0.45	0.82	Mixed (>Integrated)
PTC-7/C	8983	0.06	0.34	0.52	Mixed (>Integrated)
PTC-8/M	14370	0.09	0.45	0.83	Mixed (>Integrated)
PTC-9/M	109.4	0.001	0.37	0.58	Mixed (>Integrated)

PTC-10/C	44770	0.28	1.35	Epi	Episomal
PTC-11/C	21000	0.13	0.18	0.22	Mixed (>Integrated)
PTC-12/M	6472	0.04	0.39	0.64	Mixed (>Integrated)
PTC-13/C	555500	3.41	0.41	0.70	Mixed (>Integrated)
PTC-14/M	63.84	0.001	0	0	Integrated
PTC-15/C	2371	0.01	0	0	Integrated
PTC-16/C	5892	0.04	0.07	0.07	Mixed (>Integrated)
PTC-17/C	5647	0.03	0	0	Integrated
PTC-18/C	1123	0.01	0.06	0.06	Mixed (>Integrated)
PTC-19/C	13540	0.08	0.08	0.09	Mixed (>Integrated)
PTC-20/C	14710	0.09	0.05	0.06	Mixed (>Integrated)
PTC-21/C	25900	0.16	0.05	0.05	Mixed (>Integrated)
PTC-22/C	22740	0.14	0.07	0.08	Mixed (>Integrated)
PTC-23/C	205400	1.26	0.49	0.96	Mixed (>Integrated)
PTC-24/C	4764	0.03	0.23	0.30	Mixed (>Integrated)
PTC-25/C	56100	0.34	0.36	0.57	Mixed (>Integrated)
PTC-26/C	4061	0.02	0.27	0.37	Mixed (>Integrated)
PTC-27/M	11060	0.07	0.34	0.53	Mixed (>Integrated)
PTC-28/C	41590	0.26	0.13	0.15	Mixed (>Integrated)
PTC-29/C	241100	1.48	0.28	0.40	Mixed (>Integrated)
PTC-30/C	394500	2.43	0.34	0.51	Mixed (>Integrated)
PTC-31/S	749.1	0.005	0.65	1.84	Mixed (>episomal)
PTC-32/C	12130	0.07	0.28	0.38	Mixed (>Integrated)
PTC-33/C	100700	0.62	0.33	0.50	Mixed (>Integrated)
PTC-34/C	4.593	0.00003	1.94	Epi	Episomal
CFT-1	320.25	0.002	1.01	Epi	Episomal
CFT-2	0.759	0.00001	1.51	Epi	Episomal
CFT-3	11.16	0.00001	26.6	Epi	Episomal
SiHa	162667	1	0	0	Integrated

PTC: palatine tonsillar cancer, CFT: chronic follicular tonsillitis, C: crypt origin, S: surface origin, M: mixed crypt and surface origin, Epi: episomal

**Table 3. Physical status of HPV-16 infection in glottic cancer and tongue**

Dx/Origin	HPV-16 copies/cell	E2/E6 ratio	E2/integrated E6	Physical status
GC-1	29.82	0.42	0.42	Mixed
GC-2	13.3	1	Epi	Episomal
GC-3	1.84	1	Epi	Episomal
TC-1	4440	0.55	0.62	Mixed
TC-2	141.8	0.09	0.12	Mixed(>integrated)
TC-3	335.9	0	0	Integrated
TC-4	15.2	0	0	Integrated
TC-5	3250	0.53	0.53	Mixed
TC-6	1280	0.63	0.72	Mixed
TC-7	40.7	1.02	Epi	Episomal
TC-8	12.7	1	Epi	Episomal
TC-9	1.087	1	Epi	Episomal
TC-10	105.3	0.92	Epi	Episomal
TC-11	1129.6	0.98	Epi	Episomal

GC: glottic cancer, TC: tongue cancer, Epi: episomal

### 3. Molecular comparison according to HPV infection in palatine tonsillar cancer

On analysis of p16, skp1, survivin, cyclin A, cyclin B1, HIF-1 by immunohistochemistry, and EGFR and c-myc by fluorescent *in situ* hybridization, positive expression rates were as follows in decreasing order: 44 cases (84.62%) for cyclin B1, 43 cases (82.69%) for cyclin A, 37 cases (71.2%) for p16, 37 cases (71.2%) for survivin, 30 cases (57.69%) for skp1, 25 cases (48.08%) for HIF-1, 13 cases (25%) for c-myc gene amplification, and 7 cases (13.46%) for EGFR gene amplification (**Fig 2,3**).

Compared with HPV-negative TC, HPV-positive TC showed a strong association with p16 overexpression ( $p<0.0001$ ) and an inverse correlation with EGFR amplification ( $p=0.0478$ ). Moreover, HPV-16 integration status was

strongly associated with c-myc amplification ( $p=0.034$ ), and HIF-1 expression ( $p=0.022$ ).

Among all tested molecules and clinicopathologic parameters, p16 overexpression was significantly associated with a higher T-stage ( $p=0.0127$ ) and EGFR amplification ( $p=0.0108$ ), and it was also inversely associated with surviving expression ( $p=0.0219$ ). Skp-1 expression was strongly associated with the tumor recurrence ( $p=0.0233$ ) and cyclin A expression ( $p=0.0006$ ), but inversely associated with c-myc amplification ( $p=0.0109$ ). HIF-1 expression revealed a strong relationship with recurrence ( $p=0.0266$ ) and c-myc amplification ( $p=0.0484$ ). EGFR gene amplification and c-myc gene amplification were also strongly associated with each other ( $p=0.0132$ ).

The positive association of p16 overexpression and c-myc gene amplification with HPV infection and physical status are summarized with histological grade in **Table 4**.

**Table 4. Association of p16 and c-myc with clinicopathologic parameters**

P16	HPV (n=52)		Physical status (n=34)			Grade (n=52)		
	Neg (n=14)	Pos (n=38)	Episomal (n=3)	Mixed (n=18)	Integrated (n=13)	Well (n=16)	Mod (n=26)	Poor (n=10)
0 (n=15)	11 (21.15)	4 (7.69)	1 (2.94)	1 (2.94)	2 (5.88)	9 (17.31)	3 (5.77)	1 (1.92)
1 (n=7)	3 (5.77)	4 (7.69)	0	1 (2.94)	1 (2.94)	3 (5.77)	2 (3.85)	2 (3.85)
2 (n=7)	0	7 (13.46)	1 (2.94)	4 (11.76)	0	1 (1.92)	5 (9.62)	1 (1.92)
3 (n=23)	0	23 (44.23)	1 (2.94)	12 (35.29)	10 (29.41)	3 (5.77)	16 (30.77)	6 (11.54)
p-value	<b>P&lt;0.0001</b>		P=0.2192			<b>P=0.0426</b>		
c-myc	Neg	Pos	Episomal	Mixed	Integrated	Well	Mod	Poor
0 (n=39)	10 (19.23)	29 (55.77)	1 (2.94)	16 (47.06)	8 (23.53)	11 (21.15)	22 (42.31)	5 (9.62)
1 (n=12)	4 (7.69)	8 (15.38)	2 (5.88)	1 (2.94)	5 (14.71)	4 (7.69)	3 (5.77)	4 (7.69)
2 (1)	0 (0)	1 (1.92)	0 (0)	1 (2.94)	0 (0)	1 (1.92)	1 (1.92)	1 (1.92)
p-value	P=0.7916		<b>P=0.0340</b>			<b>P=.0360</b>		



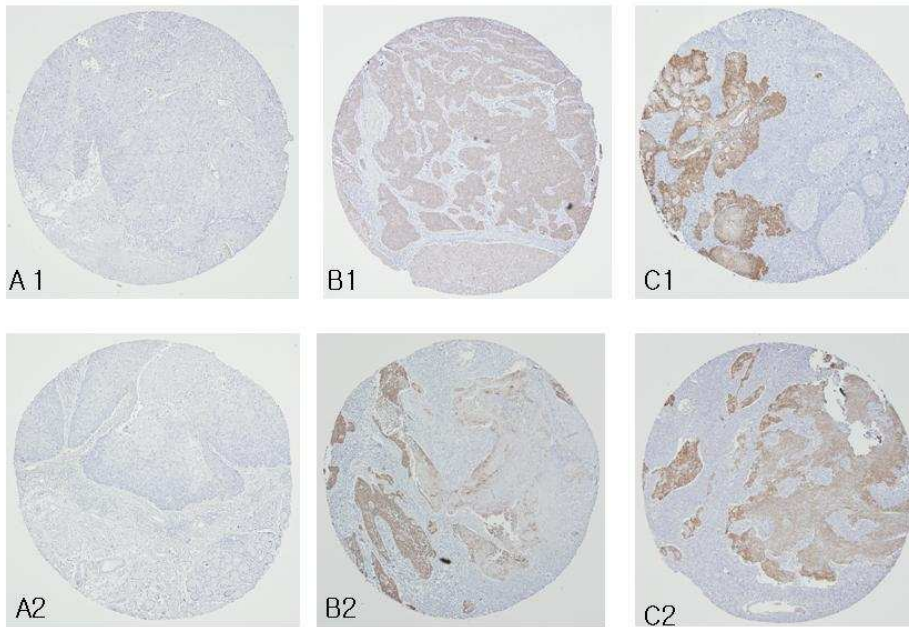


**Figure 2. Immunohistochemical results from tissue microarray.** A1 and A2: Negative staining for p16 and skp1, B1: Grade 1 staining (diffuse weak) for skp1, B2: Grade 2 staining (focal strong) for p16, C1: Grade 2 staining (diffuse strong) for skp1, C2: Grade 3 staining (diffuse strong) for p16.

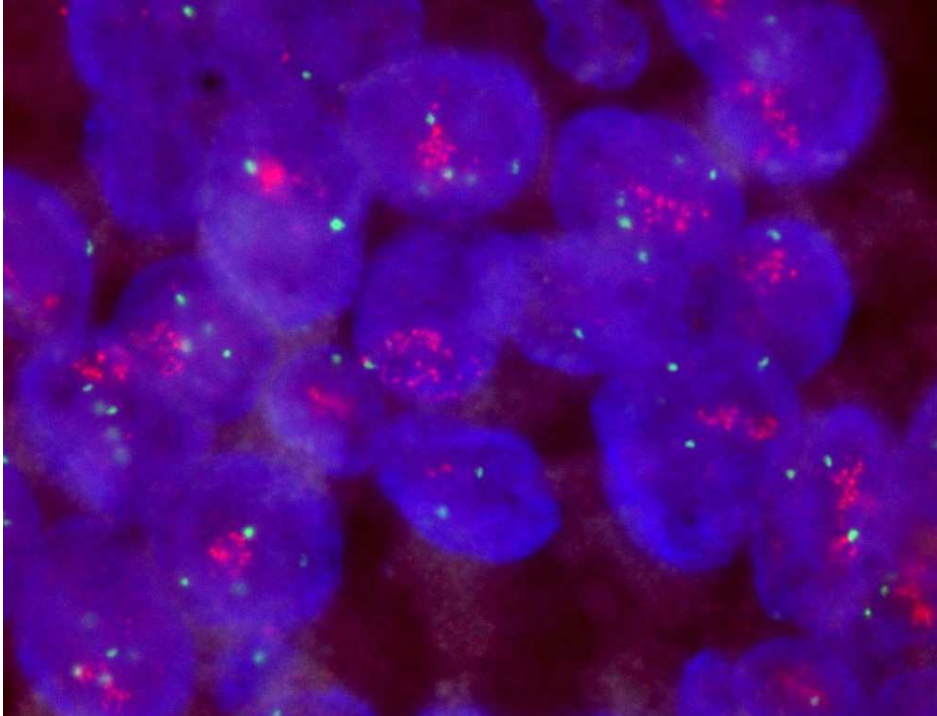


**Figure 3. Fluorescent *in situ* hybridization (FISH).** FISH shows increased c-myc gene copy numbers in tonsillar cancer (orange = c-myc; green = CEP8 control).

#### **4. Pathologic correlation according to HPV infection in head and neck cancers**

To demonstrate that HPV-associated tonsillar SCC originates from the cryptal epithelium while non-HPV-related SCC emerges from the surface epithelium, we classified the cases into 1) invaginating tumors arising from the crypt and 2) fungating or verrucous tumors directly arising from the surface, on macroscopic and microscopic reviews (Fig 4). PTCs of crypt showed a tendency for centrifugal growth (Fig. 5A), multinodularity (Fig. 5B), and occasional invasion of the surface epithelium in a pagetoid manner (Fig. 5C-D). The different phenotypes of PTCs correlated significantly with the HPV infection status ( $p < 0.0001$  by Fisher's exact test). The differentiation of the SCC was relatively

poor in the HPV-positive group ( $p= 0.0106$  by Fisher's exact test).

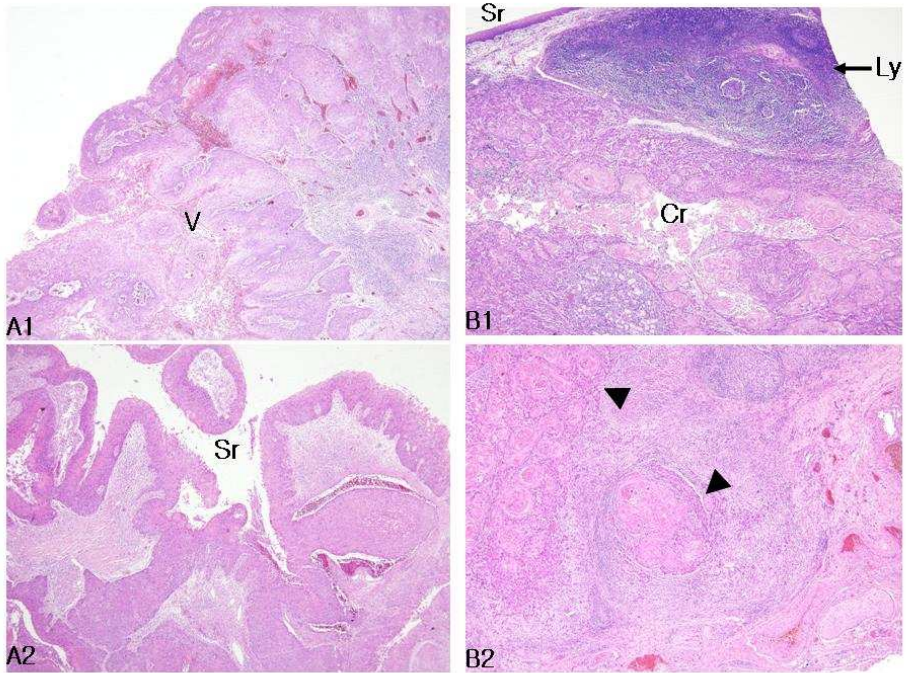


**Figure 4. Microscopic differences between tonsillar cancer of surface origin and crypt origin** A1: Verrucous or papillary changes are restricted to the surface (labeled as V). A2: Carcinomatous changes totally involve the whole tonsillar surface epithelium (Sr). B1: Papillary changes are restricted to the surface adjacent to the crypt (labeled as Cr) and densely-packed lymphoid cells (labeled as Ly). Notice a normal-looking surface epithelium (Sr) in contrast to A1. B2: A multilobulated pattern (arrowheads) of growth is characteristic of TC arising from the crypt

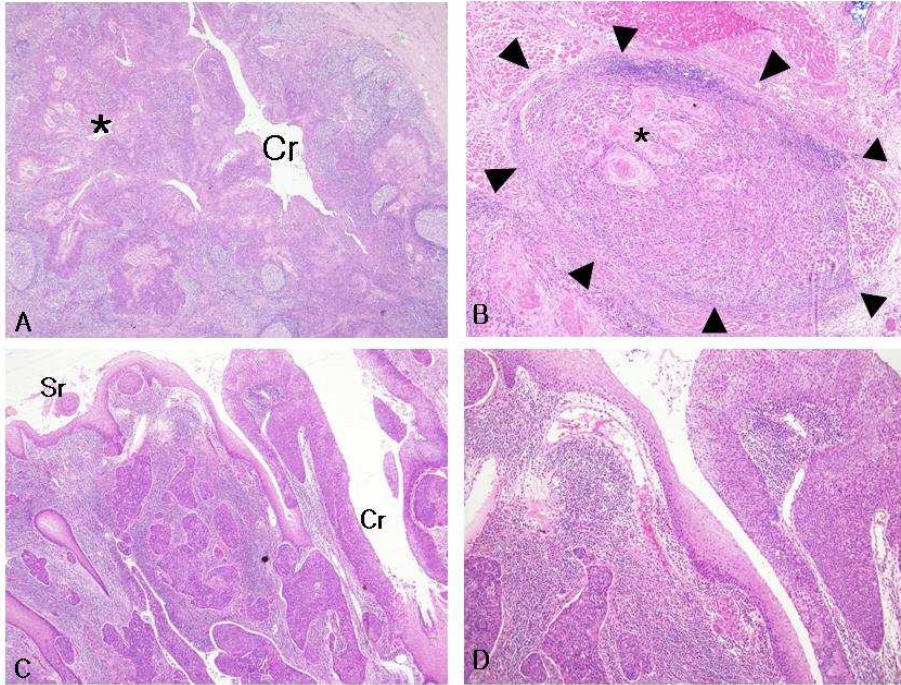


**Figure 5. Microscopic findings to suggest a crypt origin for tonsillar cancer.**

A: Early carcinoma (labeled with an asterisk) develops from the squamous epithelium lining the crypt [labeled as Cr]. B: Lobular arrangement (arrowheads) provides additional evidence of cryptal origin. Notice well-developed keratinizing pearls (asterisk). C: Underlying nested cancer tissues invade the tonsillar surface (labeled as Sr). Carcinoma *in situ* was recognized predominantly in the crypt epithelium (labeled as Cr) but spared in the surface epithelium (Sr). D: Higher magnification of carcinoma *in situ* along the cryptal epithelium

Most glottic cancers (52.1%) are in pT1 or pT2 and are well-differentiated, forming numerous keratins (69.1%). The tentacular infiltrative pattern was relatively frequent (60.9%). The involvement of the ventricle was found in 44.1% of cases, and is regarded as a sign of the transglottic cancer, pT2+ (**Fig. 2**). Vocalis muscle invasion was identified as superficial (22.3 %) or deep

(45.7%) muscle invasion (half of the whole muscle thickness) (**Fig. 3**). Thus, the incidence of pT1 with no ventricle or vocalis muscle invasion was 37.2%. Invasion to the thyroid cartilage was variably shown as minor cortical erosion (pT3), permeative growth into the medulla, direct destruction of bony cartilage, or near total replacement of cartilage (**Fig. 4**). However, there was no significant association of HPV infection with tumor gross type, volume, degree of extension to ventricle or false cord, extension of vocalis muscle, or thyroid cartilage.

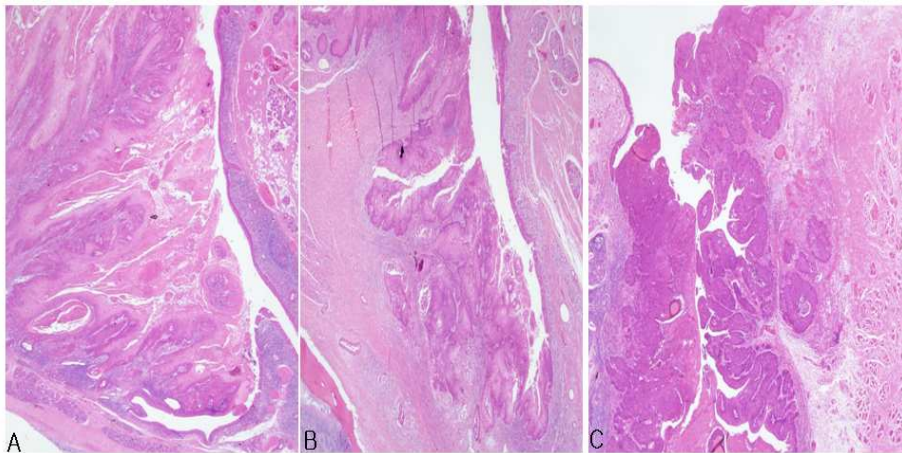


**Figure 6. Histopathologic findings associated with vocal cord motility or fixation.** A: Verrucous carcinoma is confined to the true cord, which is pT1. B: The tumor spreads along the floor of the ventricle, but not to the false cord, which favors pT1. C: The tumor extends to the false cord across the ventricle, which is compatible with pT2.

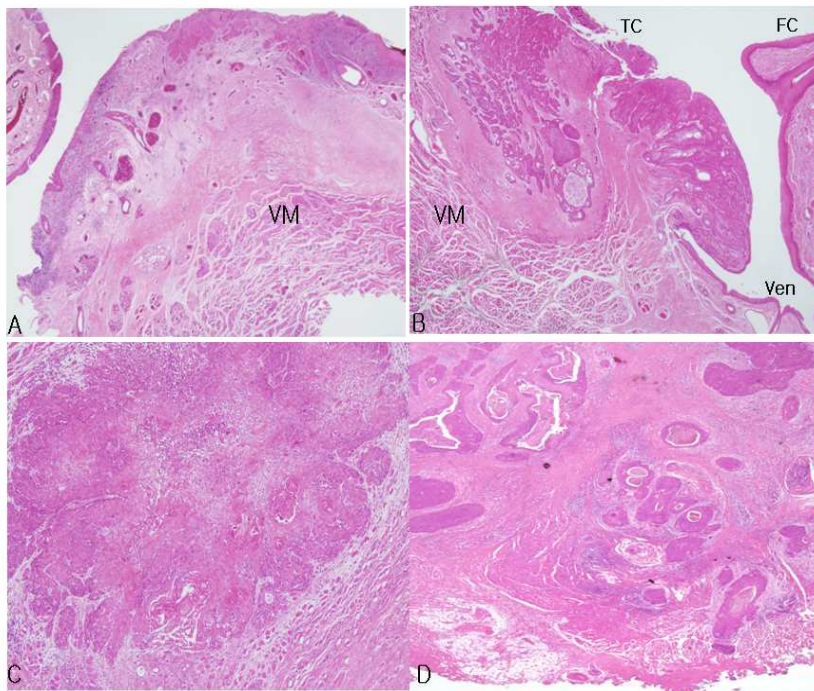


**Figure 7. Invasive depth of glottic carcinoma.** A: Glottic carcinoma confined to the superficial submucosal space. B: The tumor extends to the deep submucosal space, but not to the vocalis muscle. C: The tumor infiltrates the vocalis muscle. D: The tumor spreads to the paraglottic fat tissue.

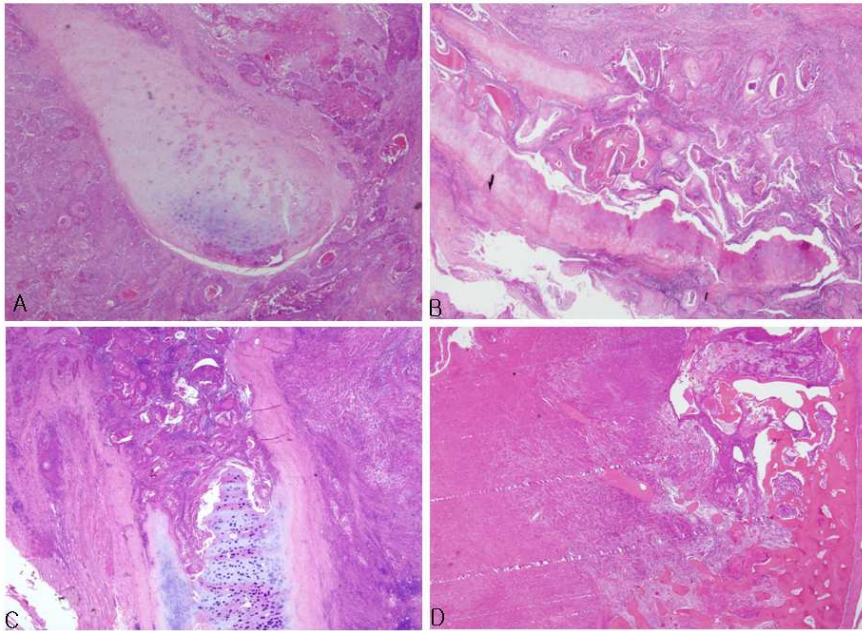


**Figure 8. Invasive pattern in the thyroid cartilage with glottic cancer.** A: The tumor surrounds the thyroid cartilage, and shows erosion of the epichondrium. B & C: The tumor directly invades the cartilage. D: The tumor completely destroys the whole thyroid cartilage

Tongue cancers in our study were entirely composed of early-onset tumors; the incidence of pT1 (less than 2 cm of superficial dimension) was 30.5% and of pT2 (less than 4 cm) was 69.5%. Tumor invasion into the underlying musculature presented as a tentacular or expansile pattern (**Fig. 9**). Occasional lymphovascular and perineural invasion were noted even in the superficial invasion (**Fig. 10**). Considering the ratio of vertical dimension relative to horizontal width, cases with deeper invasion (ratio more than 1), modest vertical invasion (less than 1 and more than 0.5), and superficial invasion (less than 0.5) were 25%, 50%, and 25%, respectively. HPV infection in tongue cancers showed a significant association with shallower infiltration to the stroma

(*p*-value= 0.032, Fig. 11). Considering just the vertical dimension, muscle invasion less than 5 mm was significantly associated with HPV infection (*p*=0.028).

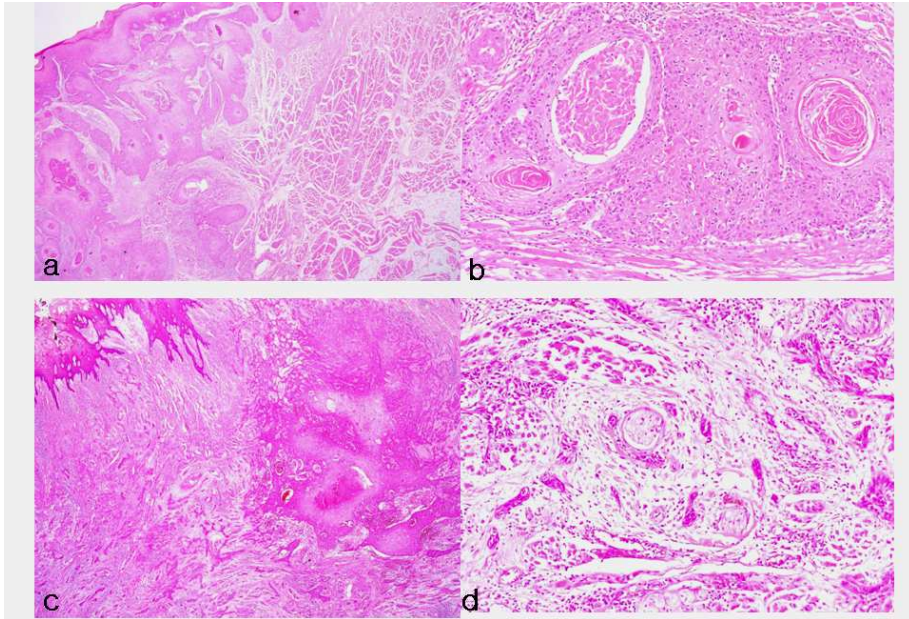


**Figure 9. Invasive pattern in the stroma with tongue cancer.** A: The tumor infiltrates into the underlying intrinsic musculature with a tentacular growth. B: The tumor infiltrates with an expansile growth pattern. C: A mixed pattern of tentacular and expansile growth is occasionally seen. D: The slender infiltrative short cords were seen with marked desmoplasia.



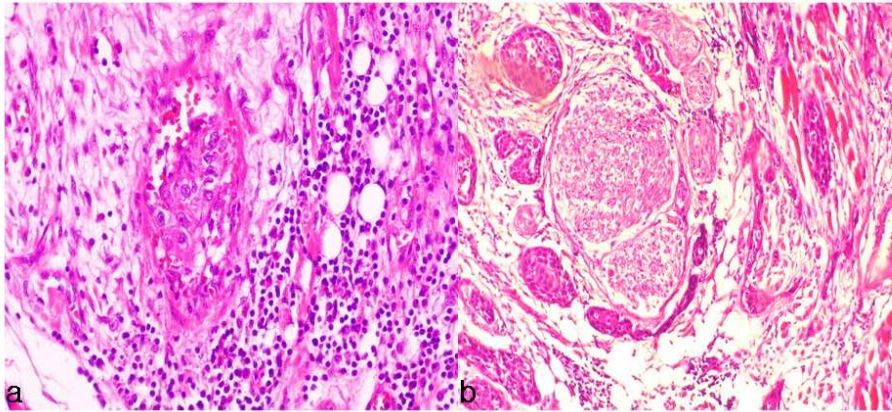


**Figure 10. Lymphovascular and perineural invasion in early-onset tongue cancer.** A: Lymphovascular invasion is identified. B: Remarkable perineural invasion is seen.

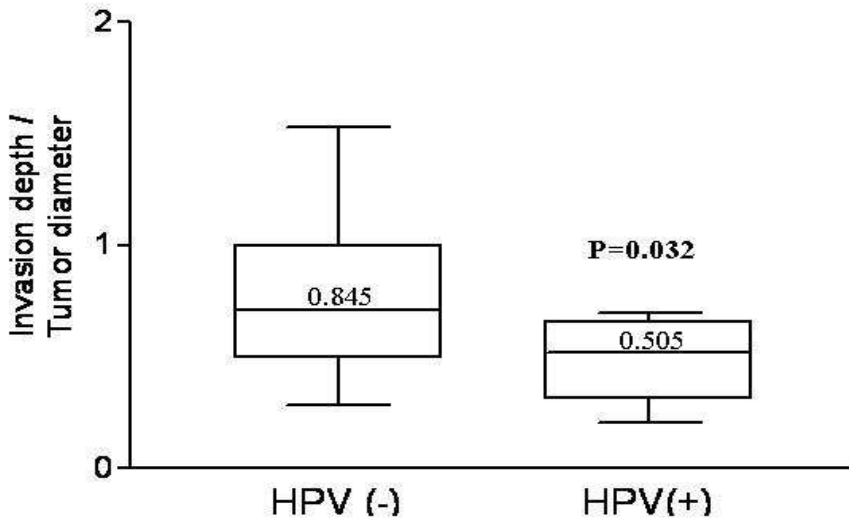


**Figure 11. Comparison of invasion characteristics according to HPV infection in the early stage of tongue cancer.** The ratio of vertical invasion to the horizontal width was significantly low in patients with HPV infection ( $p=0.032$ ).

## 5. Clinical correlation according to HPV infection in head and neck cancers

Ominous clinical findings in PTC, including death, T-stage 4, N-stage 3, M-stage 1, and recurrence were observed more frequently in the HPV-16 of non-episomal (integrated and mixed) physical state, but these findings were not statistically significant except for the N-stage ( $p < 0.0001$  by Fisher's exact test). There was no significant difference in survival between the HPV-negative group and the HPV-16-positive group (survival rates of the HPV-negative group vs. HPV-16 episomal group vs. HPV non-episomal group: 61.5% vs. 100% vs. 75%, respectively). In the cases of TC, HPV infection was significantly associated with favorable tumor-specific survival ( $p\text{-value} = 0.034$ , Fig. 12). Cases of GC showed no significant association with any clinical implication.

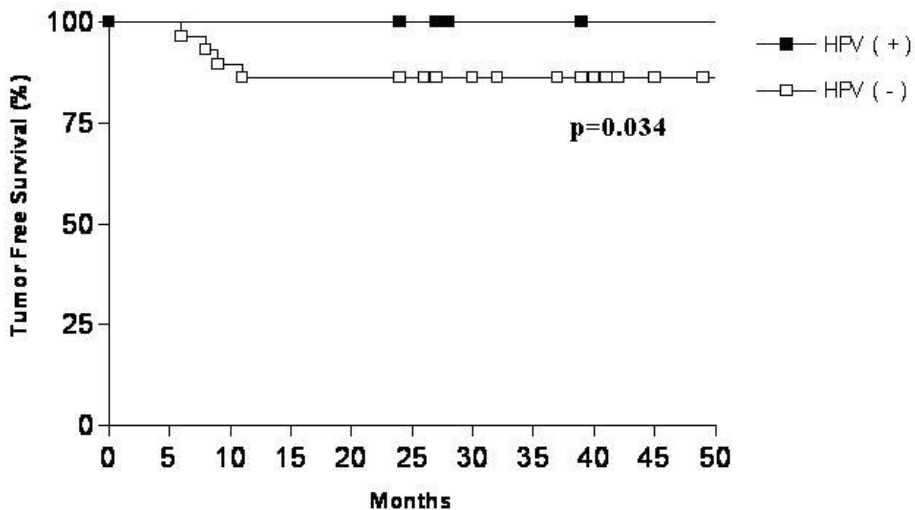


**Figure 12. Comparison of tumor-specific survival according to HPV infection.** HPV infection showed significantly favorable disease-specific survival ( $p = 0.034$ ).

## IV. DISCUSSION

The key risk factors for head and neck cancer worldwide include tobacco smoking, alcohol abuse, and especially a combination of these two.<sup>19</sup> The exact prevalence and role of human papillomavirus infection in head and neck cancer remain unknown.

In a recent epidemiologic study of 432 PTC cases, PTC showed the strongest association with HPV with an overall detection rate of 51%, with HPV-16 being the most prevalent type (84%).<sup>1</sup> With regard to oral cancer, in one of the largest multi-center case-control oral cancer studies, the incidence of HPV infection was 3.9% in 766 oral cavity cancers and 18.3% in 142 oropharynx cancers.<sup>20</sup> Despite the inconsistency among HPV DNA detection methods with a wide range of data variation,<sup>21-22</sup> the cumulative incidence of larynx cancer associated with HPV is 25.0% (313/1252).<sup>20</sup> In the present study, HPV was detected in 73.1% (38/52), 10.5% (10/95), and 36.1% (13/36) of the PTC, GC, and TC patients, respectively. In contrast to other meta-analysis or cumulative studies based on genotype-specific PCR or other classic methods, our study was performed using an HPV DNA chip with 26 different probes for HPV genotypes,<sup>11</sup> which is a highly sensitive and specific tool with high throughput, incorporating state-of-the-art technology. In the other archival data on 5,046 patients from 60 studies of head and neck cancers,<sup>23</sup> the overall HPV prevalence was 25.9%, which was significantly higher in oropharyngeal cancers than in oral (23.5%) or GC (24%). The overall HPV prevalence in the present study was 31.7% which is comparable to the HPV frequency data from other studies.

Of the HPV-positive tumors in head and neck cancer, HPV-16 is the single most common type. According to Kremier et al.,<sup>23</sup> HPV-16 accounts for the majority of HPV-positive oropharyngeal, oral and laryngeal cancers (86.7%,

68.2%, and 69.2%, respectively). In the present study, The frequency of HPV-16 was 84.5% of all HPV-positive head and neck cancers. The remaining types were infected by non-16 high-risk types, such as HPV-18, 33, 35, and 58. GC and TC were occasionally associated with the low risk genotypes, 6 or 11, whereas none of the PTC patients were infected with a low-risk HPV type.

The physical state of HPV in SCC has been analyzed with ease and reproducibility using real-time PCR, state-of-the-art technology. Our data showed HPV-16 integration in 94.1% of HPV-16 positive PTCs, with 41.2% having complete integration and 52.9% having a mixture of integrated and episomal forms. In the cases of TC, 54.5% had HPV-16 integration. However, all but one GC showed the episomal status of HPV-16. This site-specific difference in the physical state of HPV-16 is suggestive of either a direct or indirect role in carcinogenesis. Integration of HPV DNA in key points of the cell genome could cause carcinogenesis by an alternative mechanism, unrelated to early gene transcription, by blocking the transcription of tumor suppressor genes or activating protooncogene transcription.<sup>24</sup> We suggest that while HPV infection might be coincidental during the ongoing process of TC and GC, it may have a direct role in the oncogenesis of PTC and TC.

A recent paper regarding the physical status of HPV using restriction enzyme digestion, ligation and inverse PCR methods reported that all detected forms of HPV from 11 samples of 22 TCs (50%) were episomal.<sup>25</sup> Venuti et al. found that 20% of HPV-16 existed in the integrated form in laryngeal carcinomas.<sup>26</sup> However, most of the squamous cell carcinomas in head and neck cancers have indicated that HPV-DNA is more frequently integrated. Koskinen et al. reported that 65% of the HPV-DNA are integrated or mixed (integrated and episomal) in 23 head and neck cancers.<sup>27</sup> In other sites such as the esophagus, only 8.6% (3/35) of the HPV-16-positive specimens exclusively harbored the episomal

form, whereas the remaining 91.4% were either integrated (5.7%) or a mixture of the episomal and integrated forms (85.7%).<sup>28</sup> In a large series of HPV-16-positive carcinoma patients, multiple deletions were found, with the most common deletion in the region of the E2 ORF corresponding to the protein “hinge” region.<sup>29</sup> With real-time PCR, HPV-16 has been shown to be integrated in CIN lesions, and a heavy load of integrated HPV-16 is closely associated with the rapid progression of CINs.<sup>30</sup> The high frequency of partial or total integration of HPV-16 in PTC observed in this study is similar to findings from several previous studies on cervical cancer, in which viral integration can be detected in as many as 63-100% of cases and is frequently detected together with the episomal form.<sup>31-32</sup>

The exact mechanism of HPV infection in non-genital regions is unclear, but the easy access to the tonsillar crypts and the favorable microenvironmental factors of the crypts may cause the high prevalence of HPV observed in non-genital regions. HPV DNA is detected predominantly in the epithelium lining the tonsillar crypt by *in situ* hybridization.<sup>33</sup> According to our findings, we propose that HPV-associated tonsillar SCC originates from the cryptal epithelium, whereas non-HPV-related SCC emerges from the surface epithelium. We observed that the HPV infection status was related to the characteristic gross and microscopic features of the tumors. HPV-positive PTCs tend to have invaginated (inverted), multilobulated, and centrifugally-expanding growth, whereas HPV-negative PTCs tend to demonstrate fungating (polypoid) or flat and tentacular growth. HPV-positive tumors are usually poorly differentiated with basaloid morphology.<sup>3</sup>

The glottic microenvironment may be favored by HPV since the squamocolumnar junction exists in the ventricle which is just like the transitional zone of the uterine cervix; the lining epithelium of the true cord and false cord are stratified squamous epithelium and ciliated columnar epithelium,

respectively. However, we suggest that GC is less likely to be associated with HPV infection. From the clinical viewpoint, the term “transglottic” does not refer to a specific anatomic site, and designates those tumors that cross the ventricle vertically to involve both the supraglottis and glottis.<sup>19</sup> Microanatomically, the ventricle is a sac on the floor of the ventricle that divides the true vocal cord and the false cord. The underlying stroma beneath the true cord and false cord epithelium includes the vocalis muscle and the mucoserous glands, respectively.<sup>19</sup>

In contrast to supraglottic cancer, GC is typically small when detected and is in a clinically silent area where it tends to remain localized for a long period. In late stages of the disease, it may extend to the opposite true cord, to the supraglottis and to the subglottis (transglottic) or later to the thyroid cartilage and extra-laryngeal soft tissue.<sup>19</sup> Considering the T stages of larynx cancer, T1 means that the tumor is limited to the vocal cord, T2 is when the tumor extends to the supraglottis and/or subglottis, with or without impaired vocal cord motility, T3 is when there is vocal cord fixation and/or the tumor invades the paraglottic space, with or without minor erosion on the thyroid cartilage inner cortex, and T4 means that the tumor has invaded the thyroid cartilage, and/or soft tissue of the neck.<sup>19</sup> T stage determination is based on the anatomical and functional impairment, not on the microanatomy. However, microanatomical assessment is necessary for an accurate T stage assignment. Because vocal cord motility depends on the tumor invading the vocalis muscle, superficial vocalis muscle invasion should be categorized as pT2. Since transglottic cancer, which represents the invasion across the ventricle, is also characterized as pT2, microscopic findings of ventricle invasion should be standardized for pT2. It is intriguing that we rarely see primary ventricular tumors forming a bulge beneath the false cord. Vocal cord fixation can mean full tumor invasion to the vocalis muscle, which should be categorized as pT3.

Henceforth, we will put an emphasis on the degree of vocalis muscle invasion (T2 versus T3) and ventricle involvement (transglottic versus glottic) when discriminating between pT2 and pT3. An invasion through the thyroid cartilage is compatible with pT4, whereas minor cortical erosion is merely pT3 (cortex erosion versus medulla invasion).

The pathologic T stage of tongue cancer entirely depends on the horizontal dimension, irrespective of the vertical dimension or muscle invasion. The extrinsic musculature of the tongue includes muscoli hyo-, stylo-, genio-, and palatoglossus. Invasion of the intrinsic muscle alone (musculi longitudinale superior and inferior, transverses linguae and vericalis linguae) is not considered in pT, even though the tongue musculature is well supplied with blood vessels that form numerous anastomosis, and the lymphatics drain mainly into the submandibular and deep cervical lymph nodes. On survey, early onset tongue cancers are entirely composed of pT1 or pT2, and a higher relative ratio of the vertical dimension to the horizontal width is significantly associated with a poor outcome. Regarding HPV infection, cases with HPV infection revealed less invasion of the intrinsic musculature and a more favorable disease-free survival. These findings are compatible with previous results from other studies.<sup>10, 34-36</sup> It has been suggested that patients with HPV-positive head and neck cancers have better survival rates than those with HPV-negative cancers.<sup>10,34-35</sup> Dahlgren et al. mentioned that HPV is significantly more common in base of tongue cancer than in mobile tongue cancer, and HPV has a positive impact on the disease-specific survival in patients with base of tongue cancer.<sup>36</sup>

## **V. CONCLUSION**

This study on the prevalence and mechanisms of HPV infection on head and

neck cancers, including tongue, palatine tonsil, and glottic squamous cell carcinomas in a large population, revealed a significant difference in HPV prevalence among sites. Most HPV infections were due to HPV-16 and were episomal in more than half of the PTCs and TCs, but infection was seemingly coincidental in GC. HPV infection may play a direct role in PTC pathogenesis, and is associated with a better prognosis in cases of TC.



## REFERENCES

1. Syrjanen S. HPV infections and tonsillar carcinoma. *J Clin Pathol* 2004;57:449-55.
2. Frisch M, Goodman MT. Human papillomavirus-associated carcinomas in Hawaii and the mainland. *Cancer* 2000;88:1464-9.
3. Kim SH, Koo BS, Kang S, Park K, Kim H, Lee KR, et al. HPV integration begins in the tonsillar crypt and leads to the alteration of p16, EGFR and c-myc during tumor formation. *Int J Cancer* 2007;120:1418-25.
4. Munger K, Werness BA, Dyson N, Phelps WC, Harlow E, Howley PM. Complex formation of human papillomavirus E7 proteoin with the retinoblastoma tumor suppressor gene product. *EMBO J* 1989;8:4099-105.
5. Scheffner M, Werness BA, Huibregtse JM, Levine AJ, Howley PM. The E6 oncoprotein encoded by human papillomavirus type 16 and 18 promotes the degradation of p53. *Cell* 1990;63:1129-36.
6. Zur Hausen H. Papillomaviruses in human cancers. *Proc Assoc Am Physicians* 1999;111:581-7.
7. Dong XP, Stubenrauch F, Beyer-Finkler E, Pfister H. Prevalence of deletion of YY1-binding sites in episomal HPV 16 DNA from cervical cancers. *Int J Cancer* 1994;58:803-8.
8. Swoboda A, Fabrizii V. Tonsillar carcinoma in a renal graft recipient treated with cyclosporine. *Clin Nephrol* 1993;39:272-4.
9. Hemminki K, Dong C, Frish M. Tonsillar and other upper aerodigestive tract cancers among cervical cancer patients and their husbands. *Eur J Cancer Prev* 2000;9:433-7.
10. Pintos J, Franco EL, Black MJ, Bergeron J, Arella M. Human papillomavirus and prognoses of patients with cancers of the upper aerodigestive tract. *Cancer* 1999;85:1903-9.
11. Cho NH, An HJ, Jeong JK, Kang S, Kim JW, Kim YT, et al. Genotyping of

- 22 human papillomavirus types by DNA chip in Korean women: comparison with cytologic diagnosis. *Am J Obstet Gynecol* 2003;188:56-62.
12. Peitsaro P, Johansson B, Syrjanen S. Integrated human papillomavirus type 16 is frequently found in cervical cancer precursors as demonstrated by a novel quantitative real-time PCR technique. *J Clin Microbiol* 2002;40:886-91.
  13. Kalantari M, Karlsen F, Kristensen G, Holm R, Hagmar B, Johansson B. Disruption of the E1 and E2 reading frames of HPV 16 in cervical carcinoma is associated with poor prognosis. *Int J Gynecol Pathol* 1998;17:146-53.
  14. Vernon SD, Unger ER, Miller DL, Lee DR, Reeves WC. Association of human papillomavirus type 16 integration in the E2 gene with poor disease-free survival from cervical cancer. *Int J Cancer* 1997;74:50-6.
  15. Alazawi W, Pett M, Arch B, Scott L, Freeman T. Changes in cervical keratinocyte gene expression Associated with Integration of human papillomavirus 16. *Cancer Res* 2002;62: 6959-65.
  16. Randolph B, Pai S, Wayne M, Maura L, Danish H. Detection and quantitation of human papillomavirus (HPV) DNA in the sera of patients with HPV-associated head and neck squamous cell carcinoma. *Clin Cancer Res* 2000;6:4171-5.
  17. Baker CC, Phelps WC, Lindgren V, Braun MJ, Gonda MA, Howley PM. Structural and transcriptional analysis of human papillomavirus type 16 sequences in cervical carcinoma cell lines. *J Virol* 1987;61:962-71.
  18. el Awady MK, Kaplan JB, O'Brien SJ, Burk RD. Molecular analysis of integrated human papillomavirus 16 sequences in the cervical cancer cell line SiHa. *Virology* 1987;159:389- 98.
  19. Barnes L, Tse LLY, Hunt JL, Brandwein-Gensler M, Urken M, Slootweg P, et al. Tumors of the hypopharynx, larynx and trachea: Introduction. 2nd ed. WHO histological classification of tumors of the hypopharynx, larynx and

trachea. p 108-117.

20. Syrjanen S. Human papillomavirus (HPV) in head and neck cancer. *J Clin Virol* 2005;32:59-66.
21. Rees L, Birchall M, Bailey M, Thomas S. A systemic review of case-control studies of human papillomavirus infection in laryngeal squamous cell carcinoma. *Clin Otolaryngol* 2004;29:301-6.
22. Almadori G, Cadoni G, Cattani P, Galli J, Bussu F, Ferrandina G, Scambia G, Fadda G, Maurizi M. Human papillomavirus infection and epidermal growth factor receptor expression in primary laryngeal squamous cell carcinoma. *Clin Cancer Res* 2001;7:3988-93.
23. Kremier AR, Clifford GM, Boyle P, Francesch S. Human papillomavirus types in head and neck squamous cell carcinomas worldwide: A systemic review. *Cancer Epidemiol Biomarkers Prev* 2005;14:467-75.
24. Almadori G, Galli J, Cadoni G, Bussu F, Maurizi M. Human papillomavirus infection and cyclin D1 gene amplification in laryngeal squamous cell carcinoma: biologic function and clinical significance. *Head Neck* 2002;24:597-604.
25. Mellin H, Dahlgren L, Munik-Wikland E, Lindholm J, Rabbani H, Kalantari M, et al. Human papillomavirus type 16 is episomal and a high viral load may be correlated to better prognosis in tonsillar cancer. *Int J Cancer* 2002;102:152-8.
26. Venuti A, Manni V, Morello R, De Marco F, Marzetti F, Marcante ML. Viral integration into the host genome occurred in 43% of cases of HPV-16 and in 20% of cases of HPV-6. Viral RNA expression was detected by reverse transcription-PCR only in HPV-16 positive tumors. *J Med Virol* 2000;60:396-402.
27. Koskinen WJ, Chen RW, Leivo I, Makitie A, Back L, Kontio R, et al. Prevalence and physical status of human papillomavirus in squamous cell carcinomas of the head and neck. *Int J Cancer* 2003; 107:401-6.

28. Si HX, Tsao SW, Poon CSP, Wong YC, Cheung ALM. Physical status of HPV-16 in esophageal squamous cell carcinoma. *J Clin Virol* 2005;32:19-23.
29. Kalantari M, Karlsen F, Kristensen G, Holm R, Hagmar B, Johansson B. Disruption of the E1 and E2 open reading frames of HPV 16 in cervical carcinoma is associated with poor prognosis. *Int J Gynecol Pathol* 1998;17:146-53.
30. Peitsaro P, Johansson B, Syrjanen S. Integrated human papillomavirus type 16 is frequently found in cervical cancer precursors as demonstrated by a novel quantitative real-time PCR technique. *J Clin Microbiol* 2002;40:886-91.
31. Badaracco G, Venuti A, Sedati A, Marcante ML. HPV-16 and HPV-18 in genital tumors: significantly different levels of viral integration and correlation to tumor invasiveness. *J Med Virol* 2002;67:574-82.
32. Tonon SA, Picooni MA, Bos PD, et al. Physical status of the E2 human papillomavirus 16 viral gene in cervical preneoplastic and neoplastic lesions. *J Clin Virol* 2001;21:129-34.
33. Begum S, Cao D, Gillison M, Zahurak M, Westra WH. Tissue distribution of human papillomavirus 16 DNA integration in patients with tonsillar carcinoma. *Clin Cancer Res* 2005;11:5694-9.
34. Cruz IB, Snijders PJ, Steenberg RD, et al. Age-dependence of human papillomavirus DNA presence in oral squamous cell carcinomas. *Eur J Cancer B Oral Oncol* 1996;32B:55-62.
35. Matzow T, Boysen M, Kalantari M, et al. Low detection rate of HPV in oral and laryngeal carcinomas. *Acta Odontol* 1998;37:73-6.
36. Dahlgren L, Dahlstrand H, Lindquist D, Hogmo A, Bjornestal L, Lindhorm J, et al. Human papillomavirus is more common in base of tongue than in mobile tongue cancer and is a favorable prognostic factor in base of tongue cancer patients. *Int J Cancer* 2004;112:1015-9.

< ABSTRACT(IN KOREAN)>

두경부 편평세포암종에서 해부학적 위치에 따른 인간 유두종  
바이러스의 병인론적 역할에 대한 비교 분석

<지도교수 최은창>

연세대학교 대학원 의학과

이 세 영

두경부에 발생하는 편평세포암의 전체 암 발생빈도의 6% 정도를 차지하며 암으로 인한 사망의 5% 정도를 차지한다. 이러한 두경부암의 원인으로는 담배와 술, 구강위생상태, 위식도역류등이 알려져 있지만 최근 인간 유두종 바이러스를 비롯한 바이러스가 두경부암의 원인 인자가 될 수 있다는 연구가 활발히 이루어지고 있다. 인간 유두종 바이러스는 두가닥의 환형 DNA로 이루어진 바이러스로 100가지 이상의 종류가 있으며 이중 16, 18, 31, 45가 악성 종양과 관련이 있고 주로 편평상피세포에서 종양을 유발한다고 알려져 있으며 특히, 자궁경부암의 경우 95~99%에서 인간 유두종 바이러스가 원인이라고 알려져 있다.

두경부암과 인간 유두종 바이러스 간의 관계에 대해서는 지금까지 많은 연구가 진행되어 왔으며 일부 연구에서는 편도암과 인간 유두종 바이러스 간에 상관관계가 있음이 밝혀지기도 하였으나 아직까지 두경부 종양형성에 있어 인간 유두종 바이러스의 역할에 대한 연구는 논란이 많고 명확한 결론이 내려지지 않은 상태이다. 따라서 본 연구에서는 두경부암 중 가장 흔한 편도암과 구강설암, 후두암을

대상으로 인간 유두종 바이러스의 감염 빈도와 physical status를 알아보고 이를 두경부암의 임상 양상 및 예후와 비교하여 인간 유두종 바이러스가 두경부암의 종양형성과 임상양상에 어떠한 영향을 주는지 알아 보고자 하였으며 더불어 두경부암의 위치에 따라 인간 유두종 바이러스의 역할에 차이가 있는지를 알아 보고자 하였다.

1995년부터 2005년까지 연세대학교 신촌 세브란스병원에서 편도암과 구강설암, 후두암을 진단받고 초치료로 수술을 시행받은 182예를 대상으로 하였다. 감염된 인간 유두종 바이러스의 종류를 알아보기 위해 HPV Chip genotyping을 시행하였고 physical status와 viral load number를 알아보기 위해 real-time PCR을 시행하였다. 인간 유두종 바이러스와 종양형성간의 관계를 알아보기 위해 tissue microarray를 한 후 p16, survivin, cyclin A, cyclin B1, HIF-1 $\alpha$ , skp-1에 대해 면역조직화학염색을 시행하였고 EGFR, c-myc에 대해 fluorescent in situ hybridization을 시행하였다. 그리고, 각각의 두경부 암에 대해 임상양상과 병리학적 특성을 알아 본 후 이를 비교 분석하여 다음과 같은 결과를 얻었다.

1. 인간 유두종 바이러스의 이환율은 편도암이 73.1%, 구강설암이 36.1%, 후두암이 7.4%이었으며 편도암의 경우 정상 조직에 비해 통계학적으로 유의하게 높은 감염빈도를 보였으며 구강설암과 후두암은 통계학적으로 유의한 차이를 보이지 않았다. 또한 편도암의 경우 구강설암과 후두암에 비해 통계학적으로 유의하게 높은 감염빈도를 보였다.
2. 감염된 바이러스의 종류를 알아본 결과 편도암의 경우 87.2%가 HPV-16이었으며 구강설암은 84.6%, 후두암은 60%가 HPV-16이었다. 그리고, 감염된 인간 유두종 바이러스의 physical status를 알아본 결과 편도암의 경우 94.1%가 integration

status이었으며 구강설암은 54.5%, 후두암은 33.3%가 integration status이었다.

3. 인간 유두종 바이러스에 감염된 편도암의 경우 cryptal epithelium 기원을 보였으며 감염이 되지 않은 경우는 surface epithelium 기원을 보였고 구강설암의 경우 인간 유두종 바이러스에 감염된 경우 근육 내 침습이 감염이 없는 경우보다 덜하였다. 하지만 후두암의 경우 바이러스 감염과 병리학적 소견간에 상관관계를 가지는 인자는 없었다.
4. 편도암에서 p16, EGFR의 발현이 인간 유두종 바이러스의 감염과 통계학적으로 유의한 상관관계를 보였으며 HIF-1 $\alpha$ 와 c-myc은 HPV-16 integration과 통계학적으로 유의한 상관관계를 보였다.
5. 편도암의 경우 국소 림프절 전이와 인간 유두종 바이러스 감염간에 통계학적으로 유의한 상관관계가 있었으며 구강설암의 경우 생존율과 인간 유두종 바이러스 감염간에 통계학적으로 유의한 상관관계가 있었다. 하지만 후두암에서는 인간 유두종 바이러스의 감염과 임상양상간에 통계학적으로 유의한 상관관계가 관찰되지 않았다.

결론적으로 본 연구를 통해 두경부암과 관련된 인간 유두종 바이러스는 대부분 HPV-16임을 확인하였고 편도암과 구강설암에서는 50% 이상이 intergration status임을 확인하였다. 그리고, 여러 두경부암 중 편도암에서 인간 유두종 바이러스와 종양형성이 관련이 있음을 알 수 있었으며 구강 설암에서는 인간 유두종 바이러스가 예후 인자로 사용될 수 있는 가능성이 있음을 알 수 있었다.

---

핵심되는 말 : 인간 유두종 바이러스, 편평세포암, 편도, 구강설, 후두